International Journal of Mathematical Sciences
Vol. 17, Nos. 3-4, July-December 2018, pp. 205-226
© Serials Publications

INCLINED MHD CASSON FLUID FLOW OVER A PERMEABLE CYLINDER WITH VISCOUS DISSIPATION AND CHEMICAL REACTION

Shalini Jain and Manjeet Kumari

Abstract: In this article, we have investigated inclined MHD Casson fluid flow over a permeable cylinder with viscous dissipation and chemical reaction. Variable thermal conductivity, non-linear heat source and non-linear radiation is also taken into consideration. The PDEs of momentum, heat and mass transfer has been changed into non-linear coupled ODEs by using suitable transformation. Solved by using R-K forth order shooting technique with Matlab. The effects of parameters on the velocity, heat and mass transfer are analyzed and presented with the support of graphs and tables. Local Nusselt number, local Sherwood number and skin friction coefficient are tabulated.

Keywords: Inclined magnetic field; Casson fluid; shooting technique; permeable cylinder; chemical reaction.

1. INTRODUCTION

The Casson fluid is a non-Newtonian fluid with yield stress, which is widely used for modelling the blood flow in narrow arteries. Numerous researchers have used the Casson fluid model for the mathematical modelling of the blood flow in narrow arteries at low shear rates. It has been verified by Mathematicians as well as medical researcher, are widely working on Casson nano-fluid model. Mabood et al. [1] investigated effects of thermal radiation on Casson flow. Viscous dissipation on MHD Casson fluid flow with Cattaneo-Christov heat flux examined by Ramandevi et al. [2]. Ibrahim et al. [3] proposed chemical reactive Casson nanofluid over a nonlinear permeable stretching sheet. Reddy et al. [4] analysed MHD Casson fluid flow. Malik, et al. examined the boundary layer flow of Casson nanofluid. Kumari et al. [5] investigated MHD Casson fluid in an inclined channel. Mernone et al. [6] proposed transport phenomena of a Casson fluid. Nadeem et al. [7] investigated MHD flow of a Casson fluid. Mahdy [8] examined Casson fluid due to a stretching cylinder. Boyd et al. [9] analysed of the Casson and Carreau–Yasuda non-Newtonian blood models. Kumari, et al. [10] investigated Casson fluid in an inclined channel. Sreenadh, et al. [11] examined flow of a Casson fluid. Mukhopadhyay et al. [12] studied unsteady Casson fluid flow over stretching surface. Mukhopadhyay [13-14] analysed fluid flow over a stretching porous cylinder.

Mass transfer with chemical reaction is significantly used in chemical and hydrometallurgical industries. The formation of smog represents a first order homogeneous chemical reaction. A few representative studies dealing with mass transfer in the presence of chemical reaction are Hayat et al. [15-16], Salem et al. [17], Bhattacharyya et al. [18],

Alharbi et al. [19] proposed various fluid flow model for heat and mass transfer with chemical reaction.

In the present paper, we discussed the heat and mass transfer analysis of inclined MHD Casson fluid flow over a permeable cylinder with viscous dissipation and chemical reaction.

The governing boundary layer equations are first simplified by using suitable similarity trans-formations. The resulting equations are solved using R-K forth order with shooting technique using MATLAB. Results have been obtained α for Casson fluid parameter, Prandtl number, curvature parameter, magnetic parameter, radiation parameter, chemical reaction parameter, Schmit number and suction/injection parameter on the velocity, temperature and concentration profiles, skin friction, wall temperature gradient and concentration gradient have been obtained and tabulated.

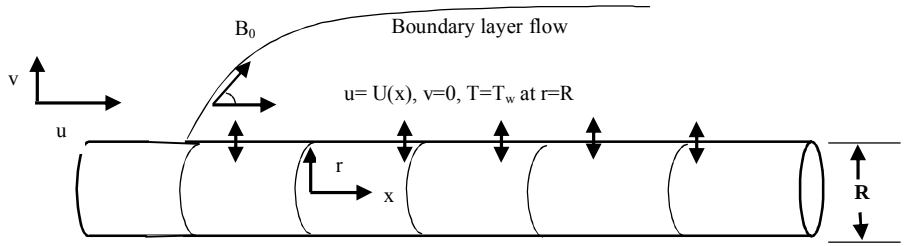

Figure 1: Schematic diagram of boundary layer flow over permeable cylinder

Table 1

Pr	*Comparison of* $-\theta'(0)$ *for different values Pr in the absence of the parameters* $S=R=Ec=M=\gamma=\lambda=\varepsilon=0$, $\alpha=\pi/2$ *and* $\beta\to\infty$					
	Nadeem et al [22]	*Khan and Pop [23]*	*Golra and Sidawi [24]*	*Wang [25]*	*Narayana et.al [28]*	*Present study*
0.7	0.454	0.454	0.454	0.454	0.4539	0.453950642
2.0	0.911	0.911	0.911	0.911	0.9114	0.911361211

Problem Statement and Mathematical Formulation

Considered the steady laminar flow of an incompressible non-Newtonian Casson fluid caused by a stretching cylinder with radius *r* in the axial direction in a fluid at rest as shown in Figure 1, where the x-axis is measured along the axis of the cylinder and the *r*-axis is measured in the radial direction. It is assumed that the surface of the cylinder is at constant temperature T_w and the ambient fluid temperature is T_∞. The viscous dissipation is considered. The continuity, momentum and energy equations are given as:

$$\frac{\partial(rv)}{\partial r}+\frac{\partial(ru)}{\partial x}=0 \tag{1}$$

$$u\frac{\partial u}{\partial x}+v\frac{\partial u}{\partial r}=\upsilon\left(1+\frac{1}{\beta}\right)\left[\frac{1}{r}\frac{\partial u}{\partial r}+\frac{\partial^2 u}{\partial r^2}\right]-\left(\frac{\sigma B_0{}^2\sin^2\alpha}{\rho}+\frac{\upsilon\phi_p}{kp}\right)u \tag{2}$$

$$u\frac{\partial T}{\partial x}+v\frac{\partial T}{\partial r} = \frac{1}{\rho c_p r}\frac{\partial}{\partial r}\left(K(T)r\frac{\partial T}{\partial r}\right)+\frac{\mu}{\rho c_p}\left(1+\frac{1}{\beta}\right)\left(\frac{\partial u}{\partial r}\right)^2-\frac{1}{\rho c_p}\frac{\partial q_r}{\partial r}+\frac{q'''}{\rho c_p} \quad (3)$$

$$u\frac{\partial C}{\partial x}+v\frac{\partial C}{\partial r} = D_B\left(\frac{\partial^2 C}{\partial r^2}+\frac{1}{r}\frac{\partial C}{\partial r}\right)-kn(C-C_\infty) \quad (4)$$

under the boundary conditions

$$u=U(x), v=-v_w, T=T_w, C=C_w, \text{ at } r=R \quad (5)$$
$$u\to 0, T\to T_\infty, C\to C_\infty \text{ at } r\to\infty$$

Here, stretching velocity $u_w=\frac{u_0 x}{l}$ and the U_0: the reference velocity l, T_∞ and T_W: respectively the characteristic length, extreme temperature and the wall temperature. On expanding T^4 in a Taylor series about T_∞ on neglecting higher order term, we get

$$T^4 \approx {T_\infty}^4+4{T_\infty}^3 T$$

$$\frac{\partial q_r}{\partial r}=\frac{\partial}{\partial r}\left(\frac{-4\sigma^*}{3k}\frac{\partial T^4}{\partial r}\right)=\frac{\partial}{\partial r}\left(\frac{-4\sigma^*}{3k}\frac{\partial({T_\infty}^4+4{T_\infty}^3T-4{T_\infty}^3T_\infty)}{\partial r}\right)=\frac{-16\sigma^*{T_\infty}^3}{3k}\frac{\partial^2 T}{\partial r^2}$$

Introduced $u=\frac{1}{r}\frac{\partial\psi}{\partial r}, v=-\frac{1}{r}\frac{\partial\psi}{\partial x}$ and the similarity transformation for the following momentum and temperature equation are defined as.

$$\eta=\frac{r^2-R^2}{2R}\sqrt{\frac{u_w}{\nu x}},\ \psi=\sqrt{U\nu x}R f(\eta),\ \theta=\frac{T-T_W}{T_W-T_\infty} \text{ and } \phi=\frac{C-C_W}{C_W-C_\infty} \quad (6)$$

$K(T)=k_\infty\left(1+\varepsilon\frac{T-T_W}{T_W-T_\infty}\right)$ (Reddy [31]), where k_∞: the thermal conductivity at a large distance away from the cylinder and ε is the small amount of thermal conductivity.

The equation (2) to (4) using the equation (6) to make a non-dimension form such as:

$$((1+2\eta\gamma)f'''+2\gamma f'')\left(1+\frac{1}{\beta}\right)-f'^2+ff''-(M\sin^2\alpha+Kp)f'=0 \quad (7)$$

$$\theta''(1+2\eta\gamma)\left(1+\varepsilon\theta+\frac{4R}{3}\right)+\Pr f\theta'+2\theta'\gamma\left(1+\varepsilon\theta+\frac{2}{3}R\right)+(1+2\eta\gamma)\varepsilon\theta'^2$$
$$+(1+2\eta\gamma)\Pr Ec f''^2\left(1+\frac{1}{\beta}\right)+A^*f'+B^*\theta=0 \quad (8)$$

$$\phi''(1+2\eta\gamma)+2\phi'\gamma - Sc\left(Kn\phi - f\phi'\right) = 0 \qquad (9)$$

Boundary conditions are given below

$$\begin{aligned} &f = S, \quad f' = 1, \quad \theta = 1, \quad \phi = 1 \quad \text{at} \quad \eta = 0 \\ &f' \to 0, \quad \theta \to 0, \quad \phi \to 0 \quad \text{at} \quad \eta = \infty \end{aligned} \qquad (10)$$

The dimensionless number Pr, γ, M, R, Kn, Sc and S are respectively the Prandtl number, curvature parameter, magnetic parameter, radiation parameter, chemical reaction parameter, Schmit number and suction/injection parameter defined as

$$\gamma = \frac{1}{R}\sqrt{\frac{x\nu}{u_w}}, \Pr = \frac{k_\infty}{\mu C_p}, M = \frac{\sigma l B_0^2}{u_0 \rho}, R = \frac{4\sigma^* T_\infty^3}{k_1 k_\infty}, \mathrm{Kn} = \frac{kn\,l}{u_0}, \mathrm{Sc} = \frac{\upsilon}{D_B} \text{ and } \mathrm{S} = v_w\sqrt{\frac{l}{\upsilon u_o}}$$

The skin friction coefficient, local Nusselt number and local Sherwood number are defined as:

$$C_f = \left(1+\frac{1}{\beta}\right)\frac{\tau_w}{\rho U^2}, \qquad (11)$$

$$Nu_x = \frac{x q_w}{k(T_w - T_\infty)} \qquad (12)$$

$$Sh_x = \frac{x J_w}{D_B(C_w - C_\infty)} \qquad (13)$$

where the skin friction τ_w, the heat flux q_w and mass flux J_w on the sheet are:

$$\tau_w = \mu\left(\frac{\partial u}{\partial r}\right)_{r=R} \qquad (14)$$

$$q_w = -k\left(\frac{\partial T}{\partial r}\right)_{r=R} \qquad (15)$$

$$J_w = -D_B\left(\frac{\partial C}{\partial y}\right)_{y=0} \qquad (16)$$

The dimensionless expressions for the skin friction coefficient and Nusselt number are the following.

$$c_f \mathrm{Re}_x^{\frac{1}{2}} = \left(1+\frac{1}{\beta}\right) f''(0) \qquad (17)$$

$$\mathrm{NuRe}_x^{-\frac{1}{2}} = -\left(1+\frac{4}{3}R\right)\theta'(0) \tag{18}$$

$$\mathrm{Sh}/\sqrt{\mathrm{Re}} = -\phi'(0), \tag{19}$$

where, $\mathrm{Re}_x = Ux/\nu$: the local Reynolds number.

2. RESULTS AND DISCUSSION

Figures 2–26 represent the velocity, temperature and concentration profiles. Figures 2-4 show the influence of (M) parameter on velocity, heat and concentration profiles. As increase the (M) parameter suppress the momentum boundary layer thickness and exactly reverse effect have been observed for the heat and concentration profiles. Figures (5-7) show the impacts of (Kp) parameter on momentum, temperature and mass profiles. Rising the (Kp) parameter suppresses the momentum profile and enhancement the thermal and concentration profiles. From Figures (8-10) it is observed that for a non-Newtonian fluids, the momentum of fluid as well as the boundary layer thickness of velocity profile decreases and temperature and concentration profile increses with the increases in (β) parameter. Figures (11-13) show the impacts of (α) parameter on momentum, temperature and mass profiles. Rising the (α) parameter suppresses the momentum profile and enhancement the thermal and concentration profiles.Figures (14-16) show the impacts of (γ) parameter on momentum, temperature and mass profiles. Rising the (γ) parameter enhance the momentum profile, thermal profile and concentration profiles. Fig. 17 shows the influences of (Pr) parameter on temperature profile. As increases the (Pr) parameter, the heat profile decreases. Figures (18-21) shows the influences of (R), (Ec), (ε) and (A*) parameters on temperature profile. As increases the (R), (Ec), (ε) and (A*) parameters, the heat profile increase. Figures 22-23 show the influence of Kn and Sc parameters on concentration profile. As the increase the value of Kn and Sc parameters, concentration boundary layer thickness as well as mass profile reduce. Physically, chemical reaction increases the rate of interfacial mass transfer. Chemical reaction suppresses the local concentration, thus increases its mass gradient and its flux. It is due to the fact that Sc is the ratio of velocity to mass diffusivities which means that when Sc increases, mass diffusivity decreases and there is a reduction in mass. Figures 24-26 show the impacts of (S) parameter on momentum, temperature and concentration profiles. As the increase in the value of (S) parameter, suppress the velocity, heat and concentration profiles. Table 1 & 2 show the comparison of the present results with the existed results of Mukhopadhyay et al. [20] and Palani et al [21], Nadeem et al [22], Khan and Pop [23], Golra and Sidawi[24], Wang [25], Anderson et al. [26], Prasad et al. [27] and Narayana et.al [28]. Table 3 shows the effects on various parameter on skin friction coefficient, local Nusselt number and local Sherwood number.

Table 2

Comparison of $f''(0)$ for different values M in the absence of the parameters $S=R=Ec=\gamma=\lambda=\varepsilon=0$, $\alpha=\pi/2$ and β

M	*Anderson et al. [26]*	*Prasad et al. [27]*	*Mukhopadhyay et al. [20]*	*Palani et al [21]*	*Present study*
0.0	1.000000	1.000174	1.000173	1.00000	1.000000158
0.5	1.224900	1.224753	1.224753	1.224745	1.224744871
1	1.414000	1.414449	1.414450	1.414214	1.414213562
1.5	1.581000	1.581139	1.581140	1.581139	1.581138830
2	1.732000	1.732203	1.732203	1.732051	1.732050808

Table 3
The skin friction coefficient, local Nusselt number and local Sherwood number are following physically parameters

M	*Kp*	β	α	γ	*R*	ε	*A**	*Pr*	*Kn*	*Sc*	*Cf*	Nh_x	Sh_x
0.0											-1.64337132	0.04418008	1.81063429
0.5											-1.80616375	-0.0521564	1.80093555
1.0											-1.95281012	-0.1415962	1.79253484
	0.0										-1.75396436	-0.0208626	1.8040049
	0.5										-1.95281012	-0.1415962	1.7925348
	1.0										-2.1300973	-0.2516748	1.7827891
		0.2									-3.7890268	-0.0212150	1.8554443
		1.0									-2.2290020	-0.0609589	1.8086978
		2.0									-1.9528101	-0.1415962	1.7925348
			0.0								-1.6433713	0.0441800	1.8106342
			π/6								-1.7539643	-0.0208626	1.8040049
			π/3								-1.9528101	-0.1415962	1.7925348
				0.0							-2.1040496	0.1280642	1.9955030
				0.05							-2.0234140	-0.0911752	1.8857343
				0.1							-1.9528101	-0.1415962	1.7925348
					0.0							0.1060117	
					1.0							-0.1415962	
					2.0							-0.2152368	
						0.0						-0.1339157	
						0.2						-0.1484248	
						0.4						-0.1595413	
							0.0					0.0111134	
							0.2					-0.1415962	
							0.4					-0.2943349	
								2.0				0.6543588	
								3.0				1.0683478	
								4.0				1.4081367	
									0.0				1.4268273
									0.2				1.5878501
									0.5				1.7925348
										1.0			1.1260574
										2.0			1.7925348
										3.0			2.3817100

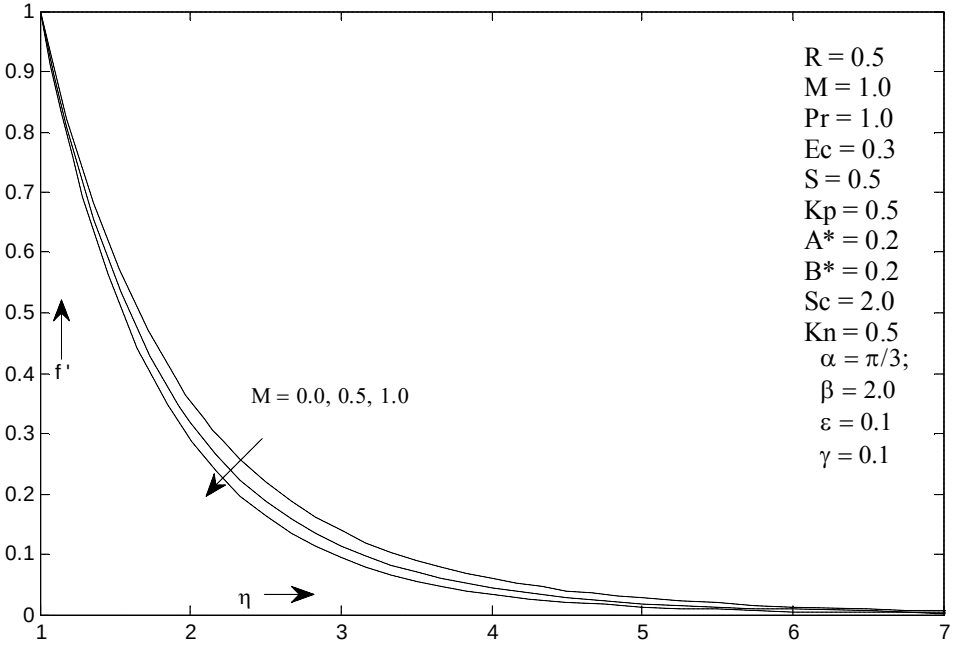

Figure 2: Impact of M on *f* ' profile

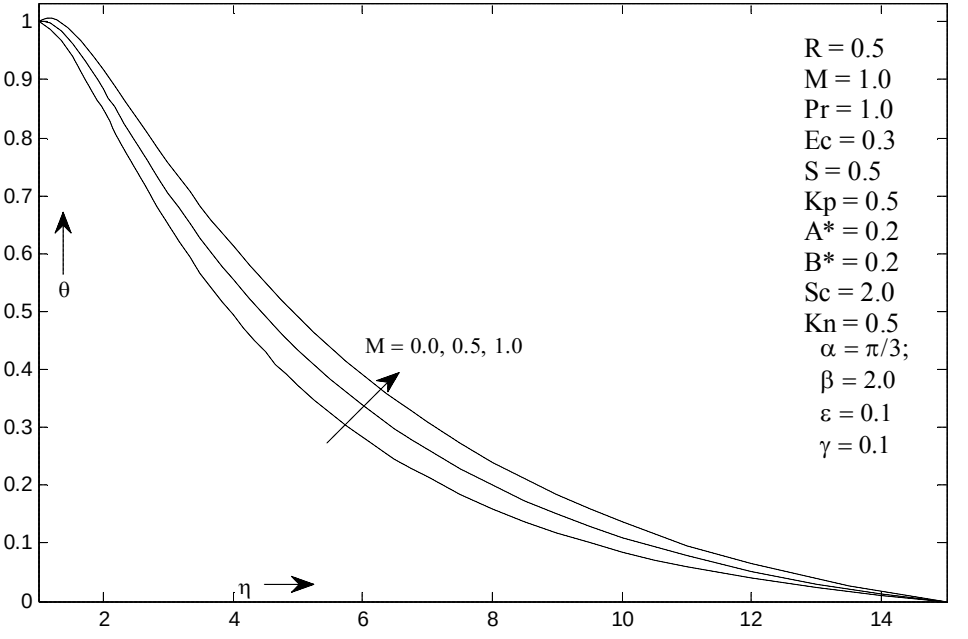

Figure 3: Impact of M on θ profile

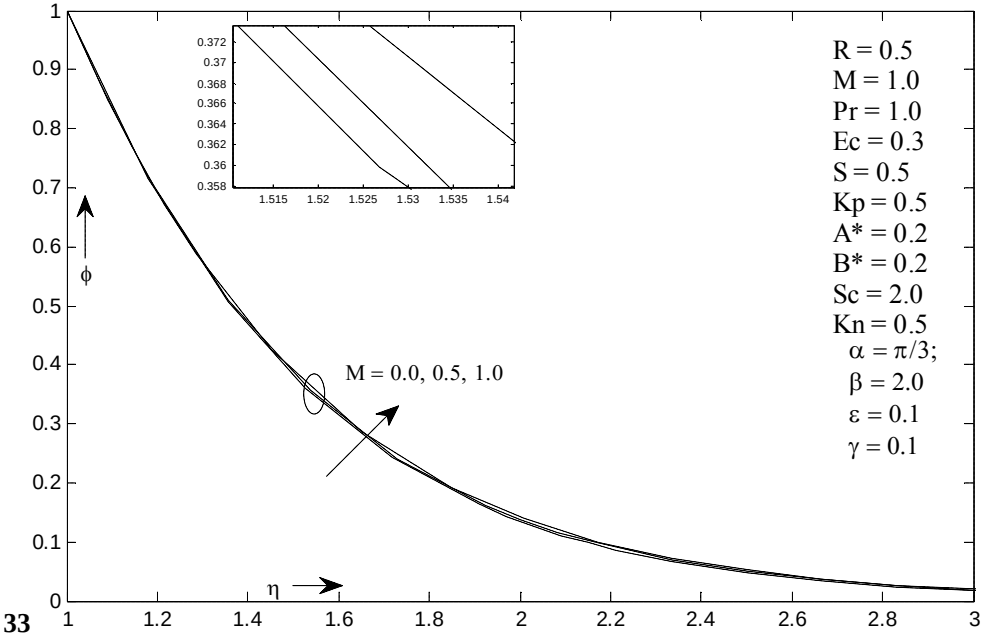

33

Figure 4: Impact of M on ϕ profile

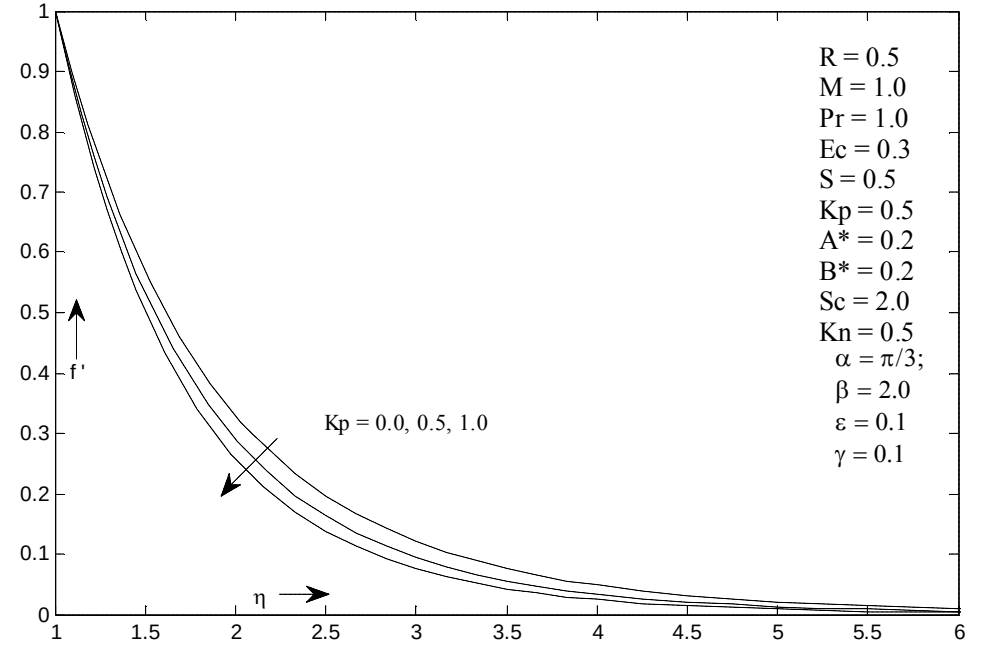

Figure 5: Impact of Kp on *f* ' profile

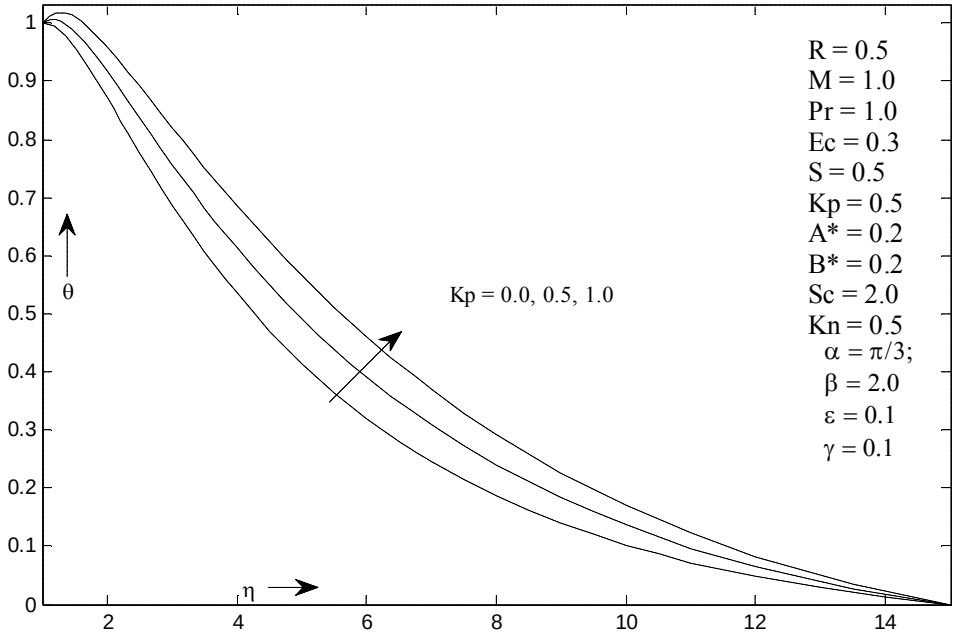

Figure 6: Impact of Kp on θ profile

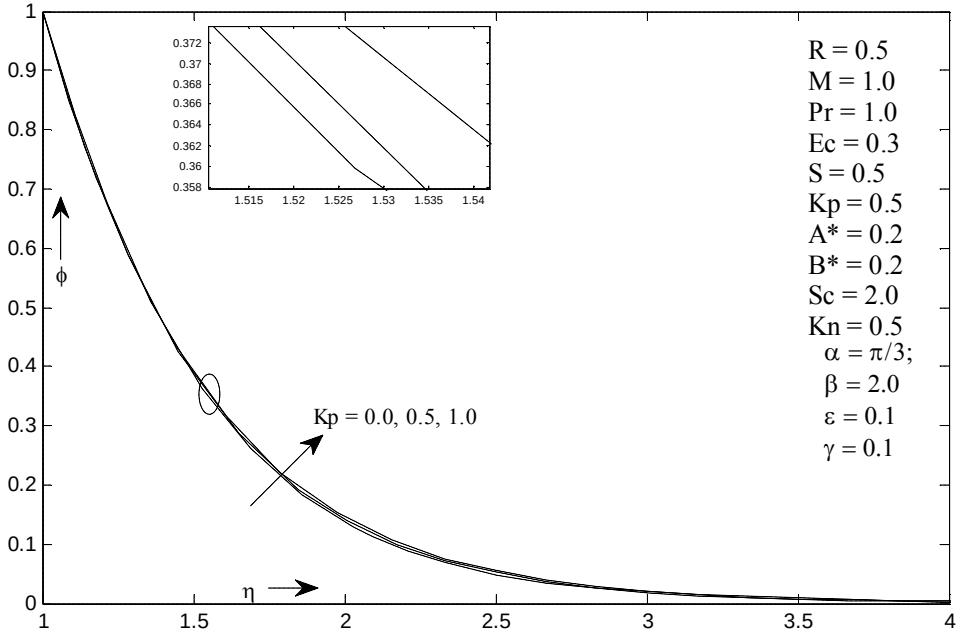

Figure 7: Impact of Kp on ϕ profile

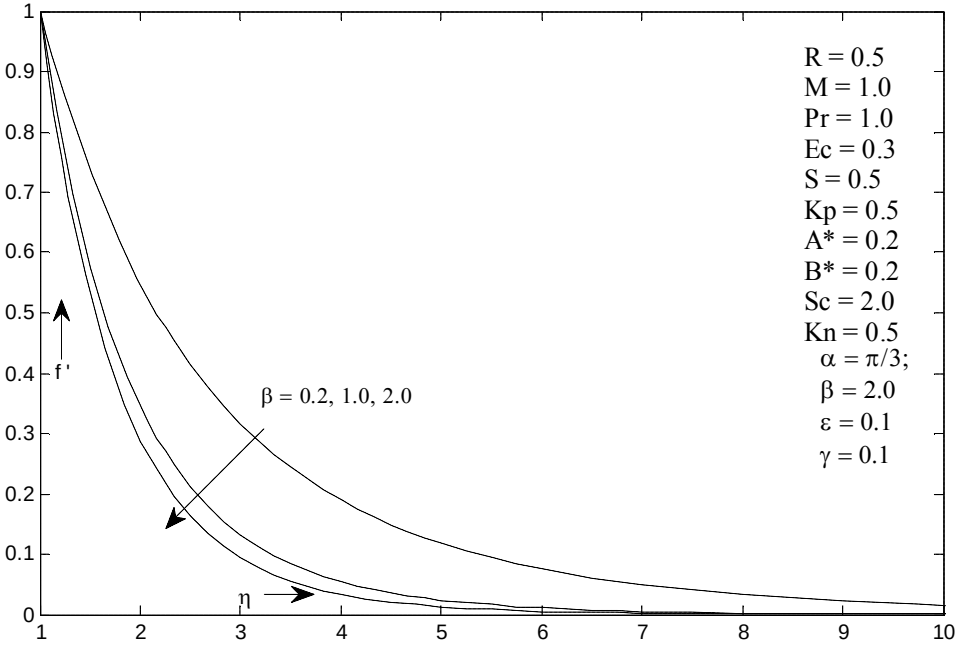

Figure 8: Impact of β on *f* ' profile

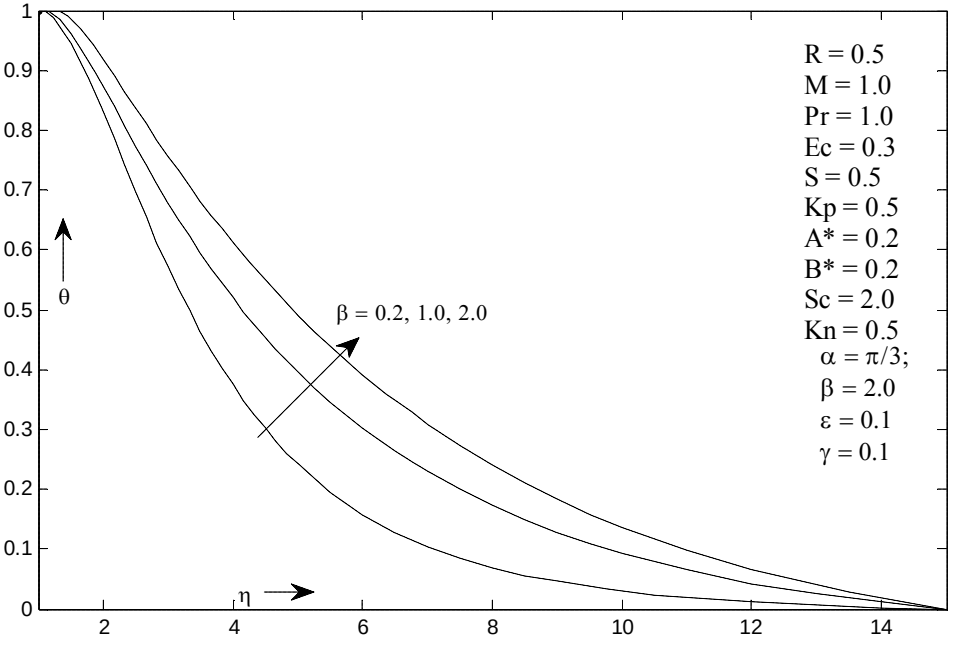

Figure 9: Impact of β on θ profile

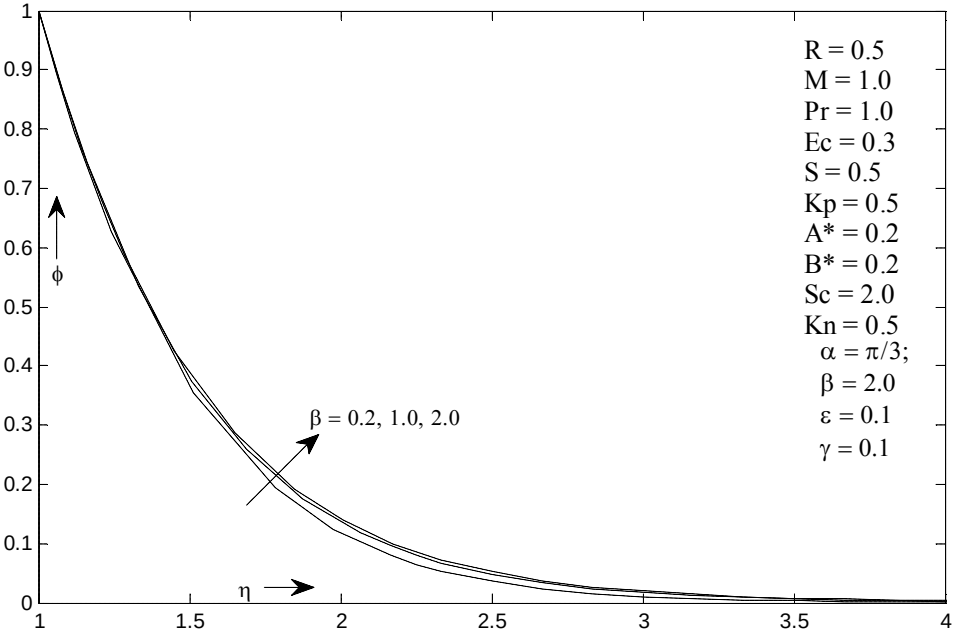

Figure 10: Impact of β on ϕ profile

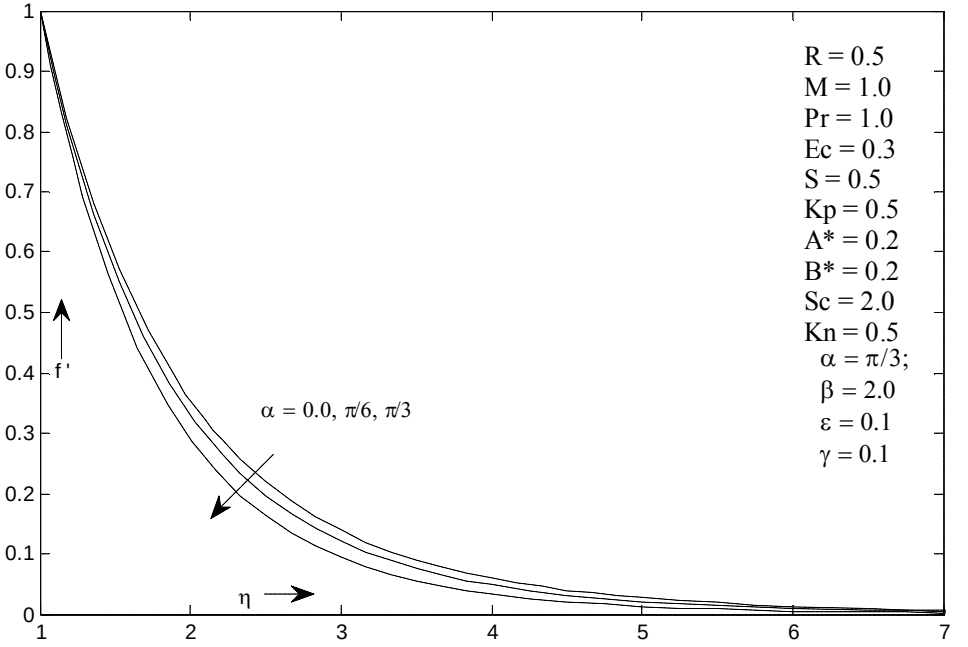

Figure 11: Impact of α on *f* ' profile

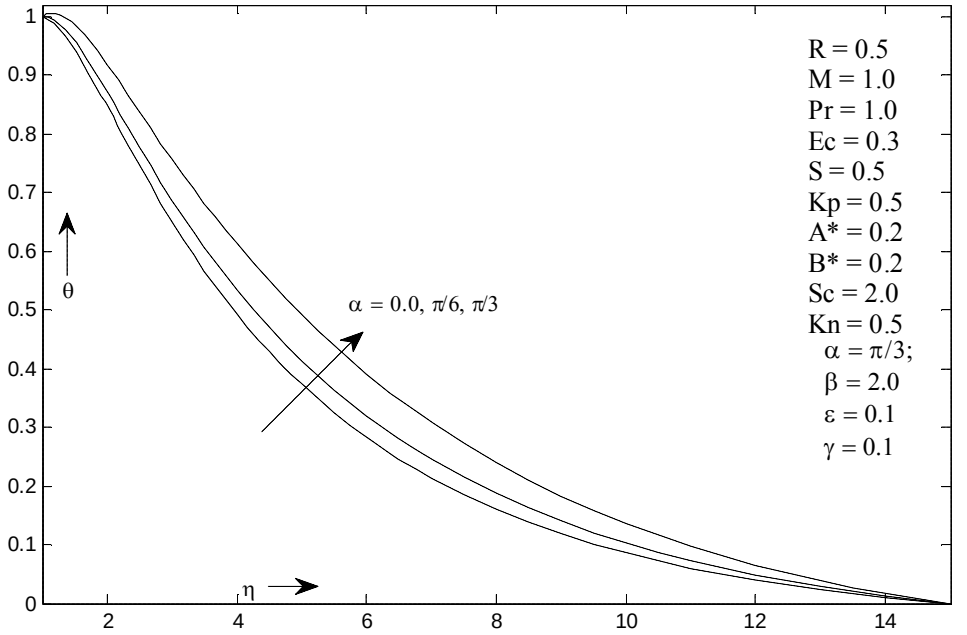

Figure 12: Impact of α on θ profile

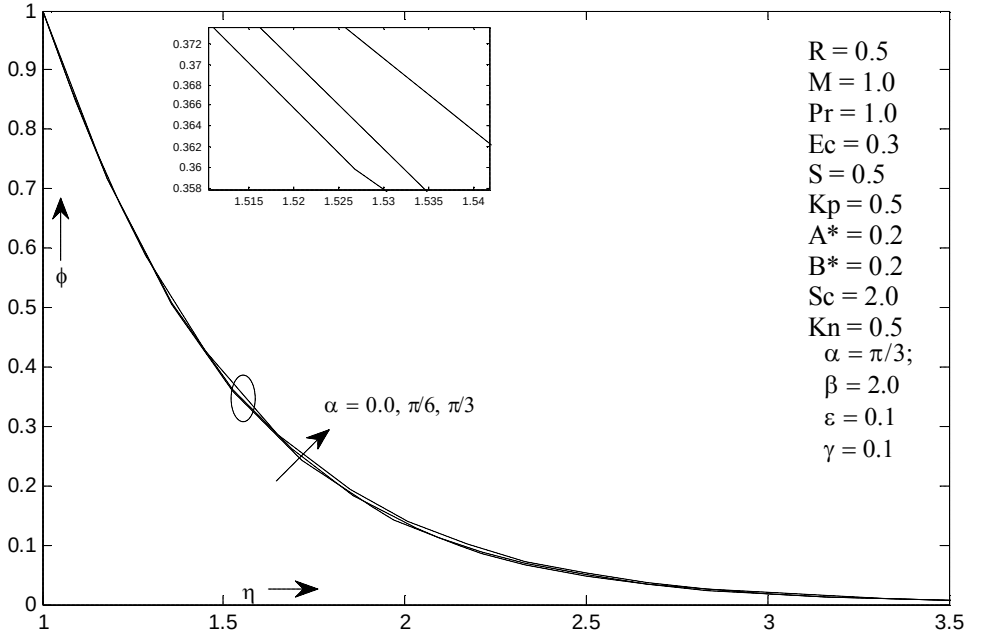

Figure 13: Impact of α on ϕ profile

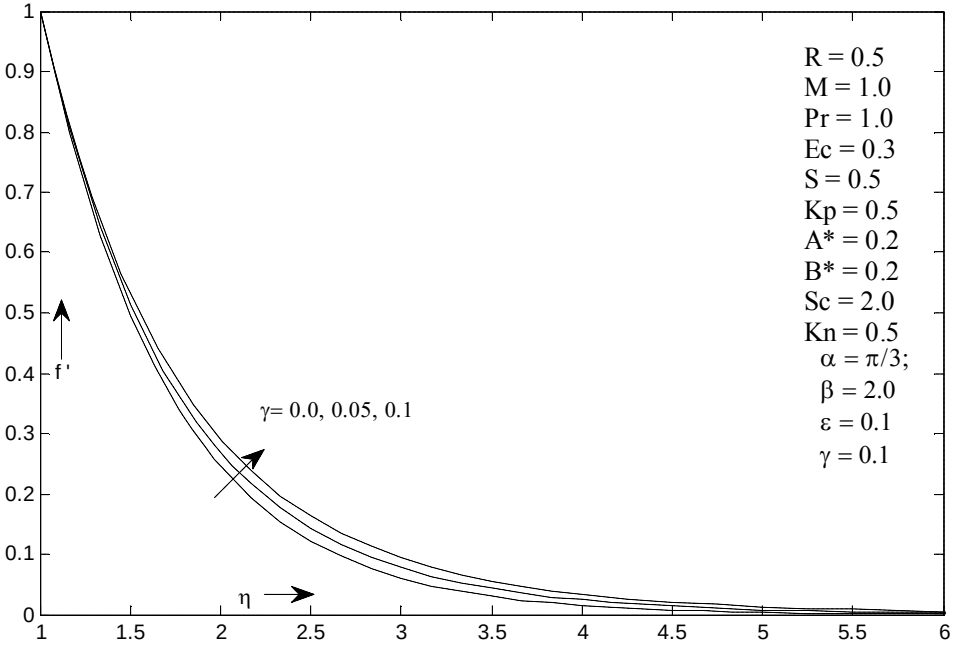

Figure 14: Impact of γ on *f* ' profile

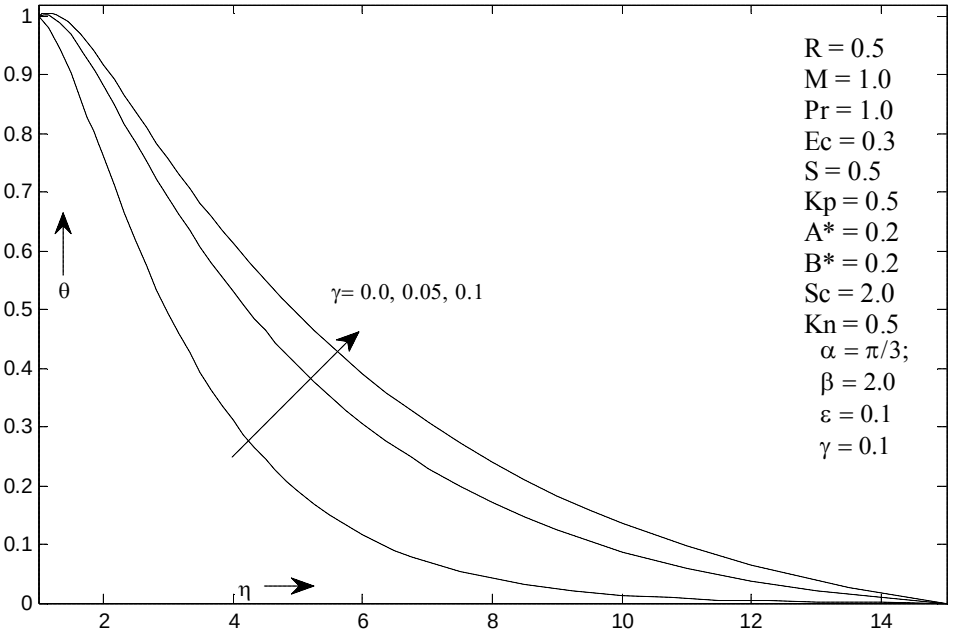

Figure 15: Impact of γ on θ profile

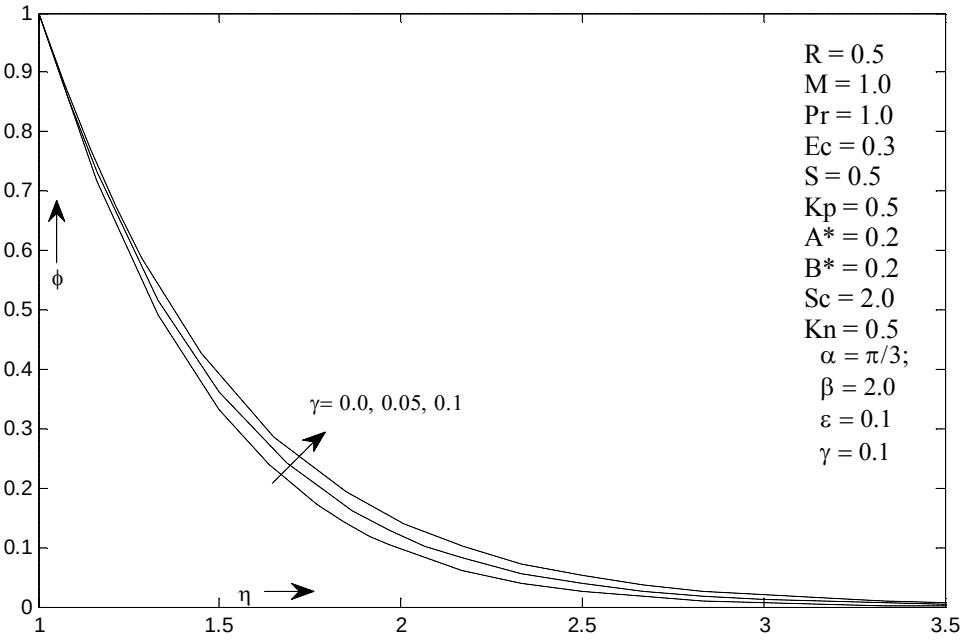

Figure 16: Impact of γ on ϕ profile

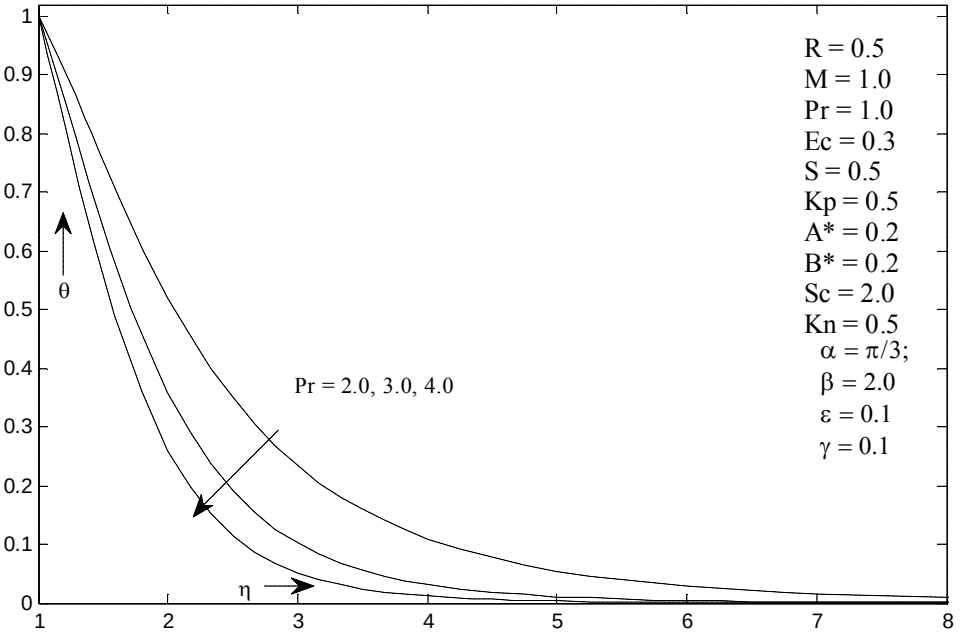

Figure 17: Impact of Pr on θ profile

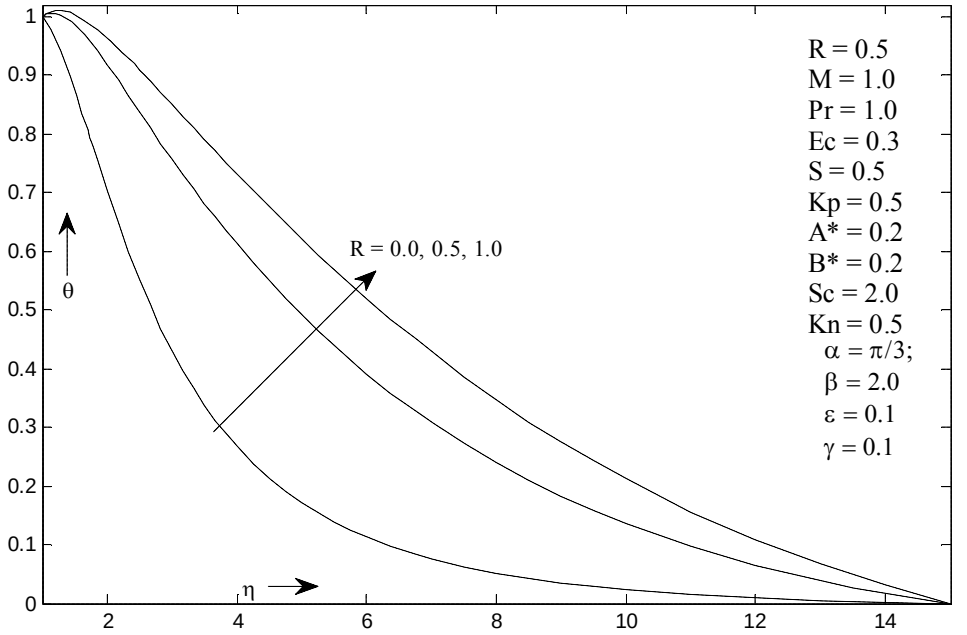

Figure 18: Impact of R on θ profile

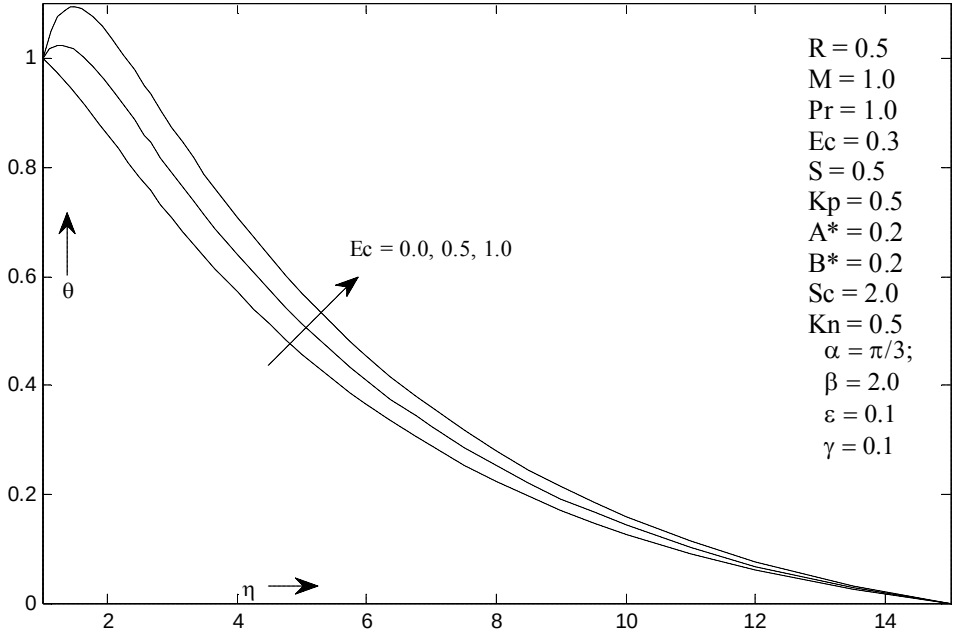

Figure 19: Impact of Ec on θ profile

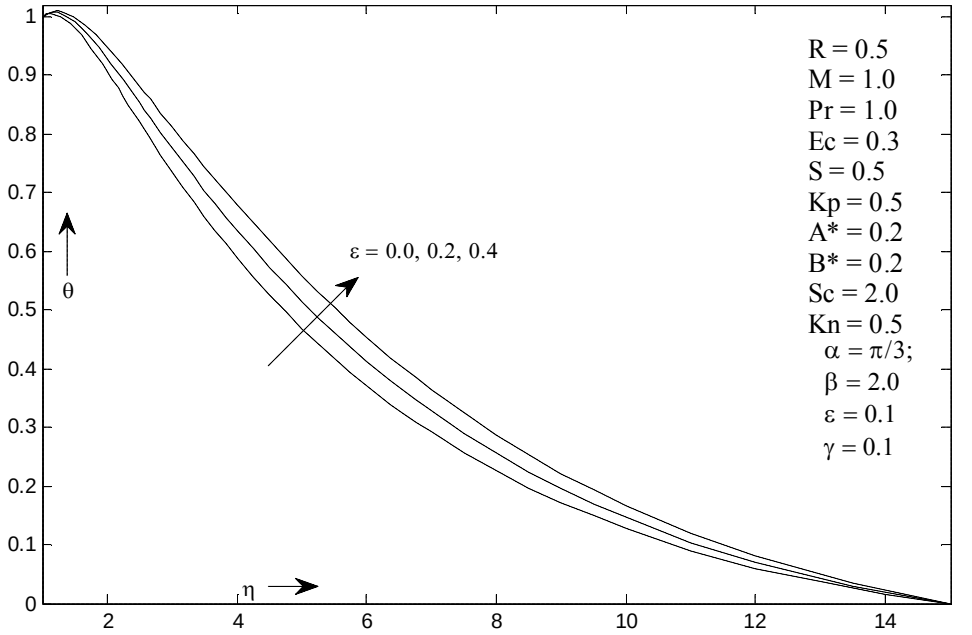

Figure 20: Impact of ε on θ profile

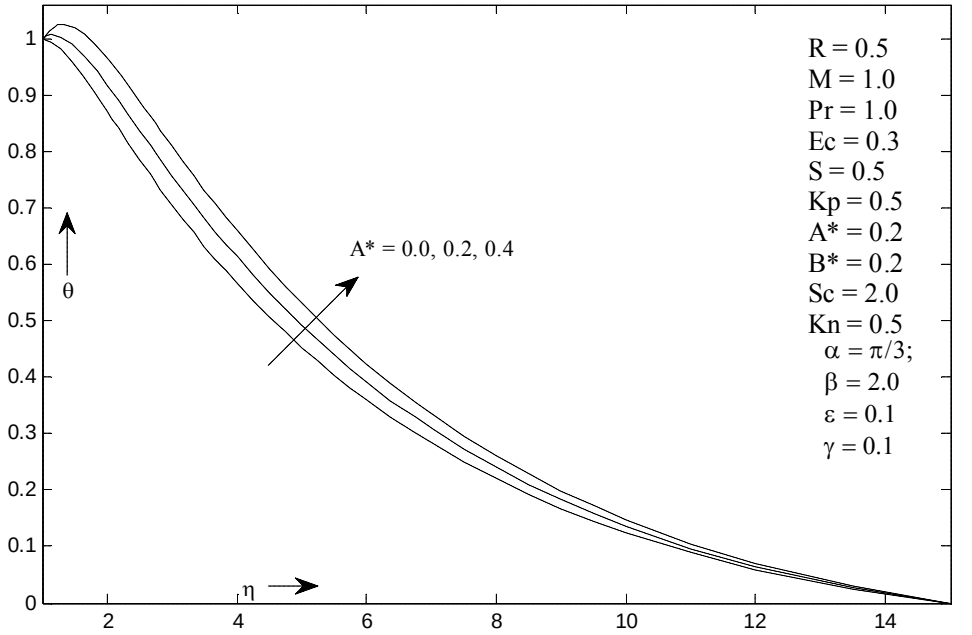

Figure 21: Impact of A* on θ profile

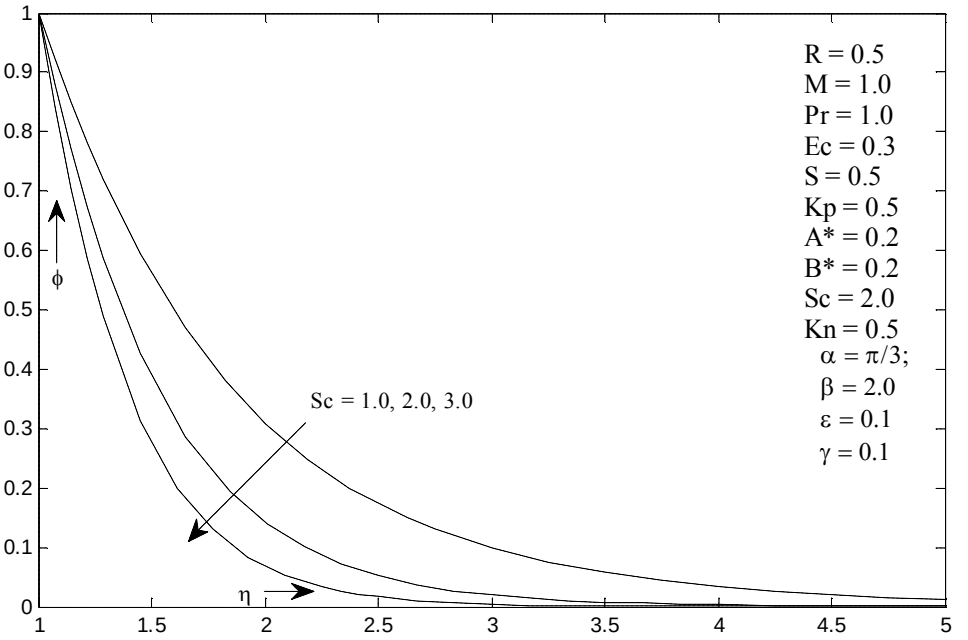

Figure 22: Impact of Sc on ϕ profile

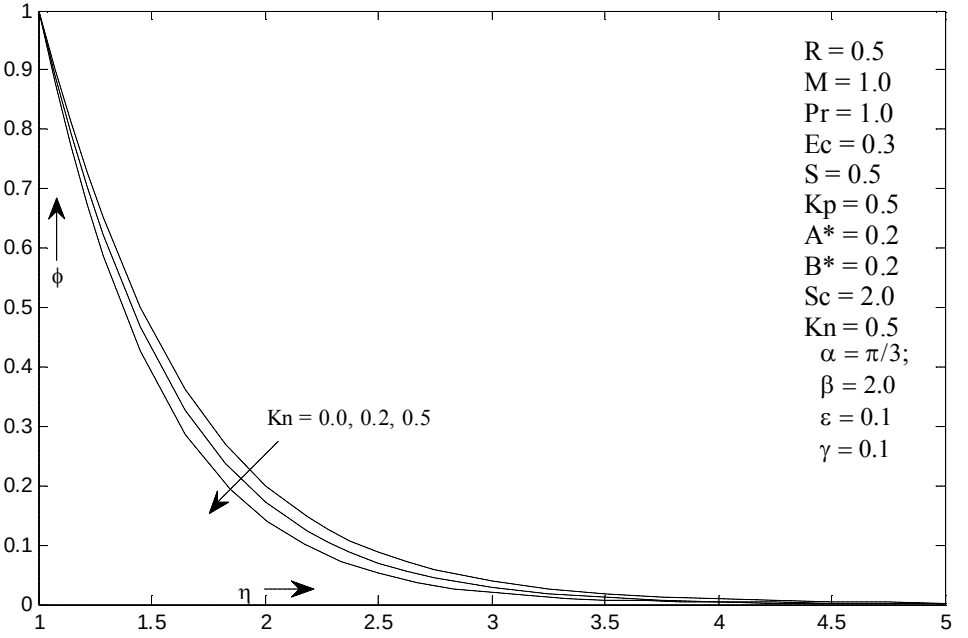

Figure 23: Impact of Kp on ϕ profile

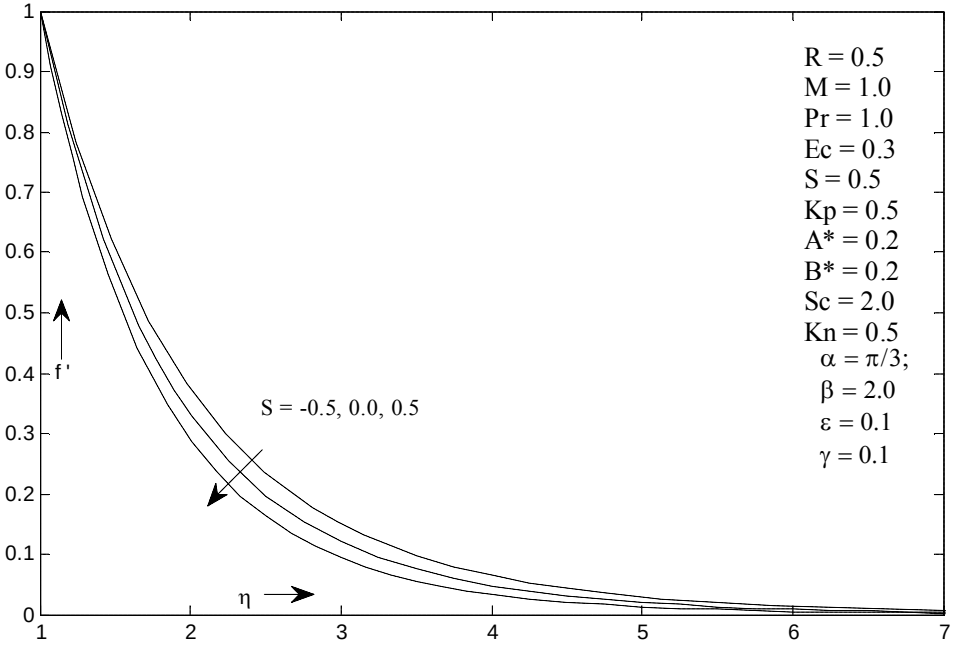

Figure 24: Impact of S on *f '* profile

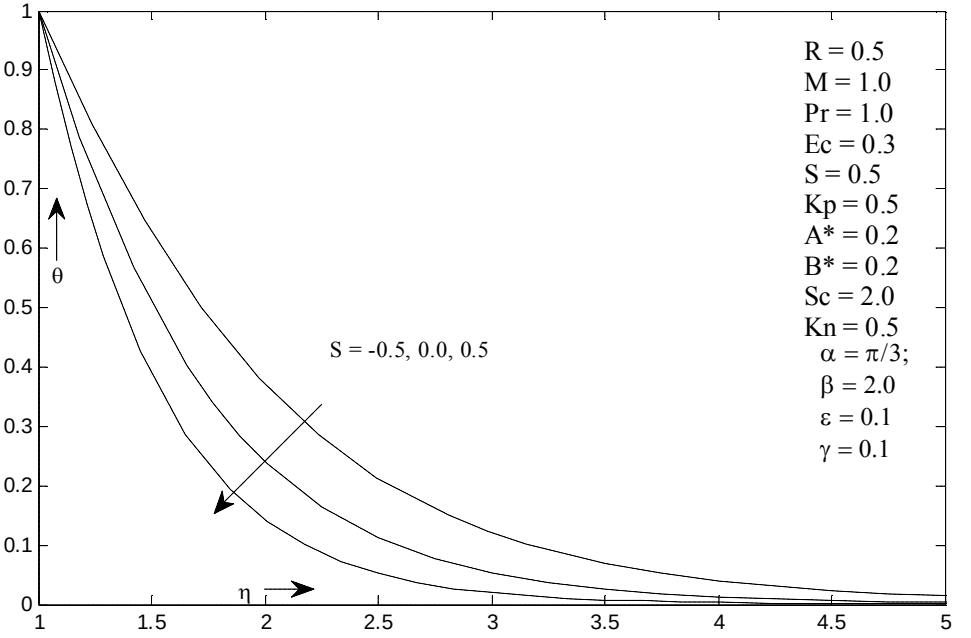

Figure 25: Impact of S on θ profile

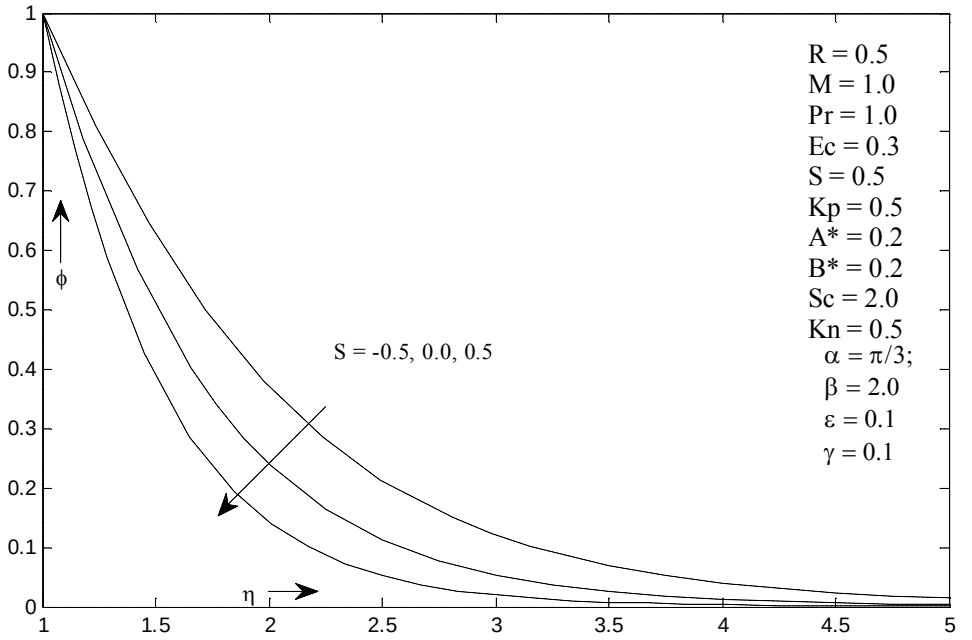

Figure 26: Impact of S on ϕ profile

3. CONCLUSION

We have discussed inclined MHD Casson fluid flow over a permeable cylinder with viscous dissipation and chemical reaction. We have considered variable thermal conductivity, non-linear heat source and non-linear radiation in temperature profile. The effects of parameters on the velocity, heat and mass transfer are analyzed with the support of graphs and tables. Local Nusselt number, local Sherwood number and skin friction coefficient are tabulated. Governing PDEs of the problem changed into nonlinear ODEs by using similarity transformation. Shooting technique with R-K 4^{th} order method is applied to find the solution of the problem. The conclusions of the present study are shown as follows:

- Increases the value of (M), (Kp), (α) and (β) suppress the momentum boundary layer thickness as well as velocity profile and opposite effects show on temperature and concentration profiles.
- Increases the value of (γ) rises momentum boundary layer thickness, heat flux as well as temperature profile and concentration profile.
- Increases the value of (R), (Ec), (A*) and (ε) rises heat flux as well as temperature profile.
- Increases the value of (Pr), suppress heat flux as well as temperature profile.

- Increases the value of (Sc) and (Kn), suppress mass flux as well as concentration profile.
- Increases the value of (γ) rises momentum boundary layer thickness, heat flux as well as temperature profile and concentration profile.

It is observed that the skin-friction increases whereas local Nusselt number and local Sherwood number decreases as the value of (β) increases.

- Skin-friction, local Nusselt number and local Sherwood number decreases as the value of (M) and (Kp) increases.

Conflict of Interests

The authors declare that there is no conflict of interests regarding the publication of this paper.

REFERENCES

[1] M. M. Hoque, N. N. Anika, and M. M. Alam, European Journal of Scientific Research 103, 343 (2013).

[2] F. Mabood, S. Shateyi, W.A. Khan, (2015). Effects of thermal radiation on Casson flow heat and mass transfer around a circular cylinder in porous medium. Eur. Phys. J. Plus., 130: 188.

[3] B. Ramandevi, J.V. Ramana Reddy, V. Sugunamma, N. Sandeep (2017). Combined influence of viscous dissipation and non-uniform heat source/sink on MHD non-Newtonian fluid flow with Cattaneo-Christov heat flux. Alexandria Engineering Journal (2017) xxx, xxx–xxx.

[4] S.M. Ibrahim, G. Lorenzini, P. V. Kumar, C.S.K. Raju (2017). Influence of chemical reaction and heat source on dissipative MHD mixed convection flow of a Casson nanofluid over a nonlinear permeable stretching sheet. International Journal of Heat and Mass Transfer, 111, 346–355.

[5] J.V.R. Reddy, V. Sugunamma, N. Sandeep, Effect of aligned magnetic field on Casson fluid flow past a vertical oscillating plate in porous medium, J. Adv. Phys. 5 (2016) 295–301.

[6] M. Y. Malik, M. Naseer, S. Nadeem, A Rehman (2014). The boundary layer flow of Casson nanofluid over a vertical exponentially stretching cylinder. Appl Nanosci., 4:869–873.

[7] Kumari SVHNK, Murthy MVR, Reddy MCK, Kumar YVKR (2011). Peristaltic pumping of a magnetohydrodynamic Casson fluid in an inclined channel. Adv Appl Sci Res 2(2):428–436.

[8] Mernone AV, Mazumdar JN (2002). A mathematical study of peristaltic transport of a Casson fluid. Math Comp Mod., 35:895–912

[9] Nadeem S, Haq RU, Lee C (2012). MHD flow of a Casson fluid over an exponentially shrinking sheet. Scientia Iranica 19:1550–1553.

[10] A. Mahdy (2015). Heat transfer and flow of a Casson fluid due to a stretching cylinder with the Soret and Dufour effects. Journal of Engineering Physics and Thermophysics, 88 (4): 928-936.

[11] J. Boyd, J. M. Buick, and S. Green, Analysis of the Casson and Carreau–Yasuda non-Newtonian blood models in steady and oscillatory flow using the lattice Boltzmann method, Phys. Fluids, 19, 93–103 (2007).

[12] P. K. Kumari, M. V. Murthy, M. Reddy, and Y. V. K. Kumar, Peristaltic pumping of a magneto hydrodynamic Casson fluid in an inclined channel, Adv. Appl. Sci. Res., 2, 428–436 (2011).

[13] S. Sreenadh, A. R. Pallavi, and Bh. Satyanarayana, Flow of a Casson fluid through an inclined tube of non-uniform cross section with multiple stenoses, Adv. Appl. Sci. Res., 2, No. 5, 340–349 (2011).

[14] Swati Mukhopadhyay, Prativa Ranjan De, Krishnendu Bhattacharyya, and G. C. Layek, Casson fluid flow over an unsteady stretching surface, Ain Shams Eng. J., 4, 933–938 (2013).

[15] S. Mukhopadhyay (2013). MHD boundary layer slip flow along a stretching cylinder. Ain Shams Engineering Journal. 4, 317–324

[16] T Hayat, M Waqas, S A Shehzad, A. Alsaedi (2016). Mixed Convection Stagnation-Point Flow of Powell-Eyring Fluid with Newtonian Heating, Thermal Radiation, and Heat Generation/Absorption, J. Aerosp. Eng., 04016077-8.

[17] S. A. Shehzad, T. Hayat, M. Qasim, S. Asghar (2013). Effects of mass transfer on MHD flow of Casson fluid with chemical reaction and suction. Brazilian Journal of Chemical Engineering. 30 (1): 187 – 195.

[18] Salem, A. M. and El-Aziz, M.A., Effect of Hall currents and chemical reaction on hydromagnetic flow of a stretching vertical surface with internal heat generation/absorption. Appl. Mathematical Modelling, 32, p. 1236 (2008).

[19] Bhattacharyya, K. and Layek, G. C., Slip effect on diffusion of chemically reactive species in boundary layer flow over a vertical stretching sheet with suction or blowing. Chemical Eng. Commun., 198, p. 1354 (2011).

[20] S. M. Alharbi, M. A. A. Bazid, M. S. El Gendy (2010). Heat and Mass Transfer in MHD Visco-Elastic Fluid Flow through a Porous Medium over a Stretching Sheet with Chemical Reaction. Applied Mathematics, 2010, 1, 446-455.

[21] Mukhopadhyay, S., Golam, A. M., Wazed, A. P.: Effects of transpiration on unsteady MHD flow of an UCM fluid passing through a stretching surface in the presence of a first order chemical reaction. Chin Phys B., 22, 124701 (2013).

[22] Palani, S., Kumar, B. R., Kameswaran, P. K.: Unsteady MHD flow of an UCM fluid over a stretching surface with higher order chemical reaction, Ain Shams Engineering Journal 7, 399–408 (2016).

[23] Nadeem, S., Hussain, S. T.: Flow and heat transfer analysis of Williamson Nanofluid" Appl Nanosci. Einstein, Ann. phys., 19, 286, (2013)

[24] Khan, W. A., Pop, I.: Boundary-layer flow of a Nanofluid past a stretching sheet, Int. J. Heat Mass Transf., 53, 2477-2483 (2010).

[25] Gorla, R. S. R., Sidawi, I.: Free convection on a vertical stretching surface with suction and blowing, Appl. Sci Res., 52, 247-257 (1994).

[26] Wang, Y.: Free convection on a vertical stretching surface, J Appl. Math Mech., 69, 418-420 (1989).

[27] Andersson, H. I., Hansen O. R., Holmedal, B.: Diffusion of a chemically reactive species from a stretching sheet, Int. J. Heat Mass Transfer, 37, 659–64 (1994).

[28] Prasad, K. V., Sujatha, A., Vajravelu, K., Pop, I.: MHD flow and heat transfer of a UCM fluid over a stretching surface with variable thermos-physical properties, Meccanica, 47, 1425–39 (2012).

[29] Narayana, K. L., Gangadhar, K., Subhakar, M J.: Effect of viscous dissipation on heat transfer of Magneto-Williamson Nano fluid, IOSR-JM., 11(4) 25-37 (2015).

[30] Hayat, T., Asad, S., Alsaedi, A.: Flow of Casson fluid with nano-particles, Appl. Math. Mech. -Engl. Ed., 37(4) 459–470 (2016).

[31] Ganji, D. D., Mustafa M. T., Sheikholeslami M.: Nanofluid flow and heat transfer over a stretching porous cylinder considering thermal radiation, IJST., 39A3 (Special issue): 433-440 (2015).

[32] Reddy, M. G.: Unsteady radiative-convective boundary-layer flow of a Casson fluid with variable thermal conductivity, Journal of engineering physics and thermophysics, 88 (1)236–246 (2015).

Shalini Jain
Dept. of Mathematics,
University of Rajasthan, Jaipur.
Email: drshalinijainshah@gmail.com

Manjeet Kumari
Dept. of Mathematics & Statistics,
Manipal University Jaipur,
Jaipur-303007, Rajasthan, India.
Email: manjeetyadav.muj@gmail.com,